Study on the evolution process of drying-wetting cycle cracks in compacted loess based on DIC technology

Changming Hu, Tingting Hu*, Yili Yuan, Fangfang Wang, Minghui Tian, and Xuhui Hou

College of Civil Engineering, Xi'an University of Architecture and Technology, Xi'an 710055, Shaanxi, China

Abstract. Loess cracks and expands easily under the condition of drying-wetting cycles, which will seriously affect the mechanical properties of loess in geotechnical engineering applications and lead to a large number of engineering accidents. Taking the loess in Yan 'an area as the research object, the drying-wetting cycles crack experimental of compacted loess was carried out by a self-made device. The surface crack of loess samples was quantitatively analyzed by using the PCAS system, and the relationship between the surface displacement, strain, and crack evolution during the drying-wetting cycles was analyzed by the digital correlation method (DIC). The results show that loess surface crack development can be divided into three stages: slow growth stage, rapid growth stage, and sluggish development stage. The displacement and strain distribution of loess surfaces are different at different positions, and the development degree of surface cracks varies with the number of drying-wetting cycles. DIC technology can be used for rapid and nondestructive detection of the displacement field and strain field on the surface of loess samples, and dynamic display of the temporal and spatial evolution characteristics of the generation and evolution of loess cracks.

1. Introduction

Loess belongs to silty clay and has some special properties. With the repeated action of climatic rainfall, loess is subjected to atmospheric forces and has the characteristics of soaking, collapsing, dehumidification and hardening. Under the action of drying-wetting cycles, it is easy to produce cracks. The existence of cracks in the loess will destroy the integrity of the loess, weaken the loess structure, and lead to engineering accidents such as slope slip and collapse. Therefore, the drying-wetting cycle is an important factor in the evolution of loess cracks.

Cracks in loess are usually presented in the form of interwoven network. In recent years, many scholars have explored the relationship between the morphological parameters of soil cracks and the drying-wetting cycle [1-3]. In the early stage, the quantitative means to obtain the geometric parameters of fracture networks usually adopt the straightedge and other tools, which cost a lot of time and labor. With the development of science and technology, more and more scholars begin to quantitatively study the development degree of soil crack through image acquisition and digital image technology. Based on the self-developed soil crack analysis system (CIAS)[4], and the MATLAB software development system [5], [6], PCAS software [7] was used to process the crack image and extract the parameters of the crack.

Due to the uncertainty of the position and direction of soil crack development, traditional measurement methods such as strain gauge, displacement meter, displacement meter, etc., cannot accurately obtain the change of soil displacement field with the crack distribution. Based on the digital correlation technique, the crack propagation process of the rock-like brittle specimen with prefabricated crack after compression is studied [8]. Combined with DIC technology, the deformation characteristics of soil around the circular anchor plate were analyzed [9]. Based on the self-developed equipment to collect soil deformation images, the DIC technology was used to analyze the local deformation of soil, and the macro failure mechanism was studied [10]. Based on DIC technology, the surface strain of soils is calculated and the process of crack generation and propagation is studied. The results show that the surface soil strain analysis can predict the crack-cracking process [11]. The strain and displacement fields in the whole process of soil shrinkage and cracking are studied based on digital correlation technology [12][13]. Through image processing and digital image correlation techniques, the changes in tracer point displacement and strain field during soil shrinkage and cracking are obtained [14][15]. At present, DIC technology is rarely reported in the field of research on cracks in the drying-wetting cycle of loess.

In this study, the whole process of loess crack evolution is dynamically monitored through an indoor drying-wetting cycle experiment and a high-resolution scanner. Combined with DIC technology, the changes of full-field displacement and strain of loess surface are analyzed and combined with quantitative indexes of loess surface crack, the evolution characteristics of the

* Corresponding author: 1072665649@qq.com

surface crack of compacted loess under drying-wetting cycles conditions are analyzed.

2. Materials and methods

2.1. Materials

The soil sample used in this study is Q_3 loess from Yan 'an city, which belongs to silty clay. Its basic physical parameters are shown in **Table 1** after the geotechnical experiment. Loess, widely distributed in northwest China, is an indispensable material in many geotechnical constructions.

Table 1. Physical parameters of the loess.

Liquid limit	Plastic limit	Plastic index	Optimal water content	Maximum dry density
29.7%	18.4%	11.3	13.5%	1.79 g/cm^3

2.2. Experimental methods

The retrieved loess samples were air-dried and passed through a 2-mm sieve, and placed in the oven at 105 ℃ for 24 h. Then add water to mix the soil, configure it to 20% saturation, and leave it for 24h. In this study, the dry density of the sample was set at 1.4g/cm^3, and the saturation was 20-100%. The group with clear fissure morphology was selected as the research object after repeated three times under the same conditions. The container used in the experiment was an acrylic mold of 220 mm×310 mm×8 mm, and the loess samples were compacted to 3 mm thick by a compacting cover plate.

A self-made drying-wetting cycle experimental device was used to carry out drying-wetting cycle crack experiments on compacted loess, as shown in **Fig. 1**. The humidification of atomized water in a pneumatic spray can be used to simulate the effect of rainfall. The constant temperature heating plate was used to ensure that the samples were kept in an environment of 30℃ to reduce the humidity. The water content of soil samples was controlled by weighing the total mass of the samples, and the accuracy could reach ±0.01g. In order to reduce the influence of external temperature and light environment in the experiment, the experiment was conducted in a dark insulation experimental chamber. A high-resolution scanner connected to a computer was placed above the soil sample close to the surface of the soil sample, and the surface image of the soil sample was scanned every 30 minutes. A thin layer of colored particles is spread evenly over the surface of the soil sample in advance.

Based on Matlab software, the cross correlation method is used to analyze the displacement field and strain field of the pictures obtained in the wet and dry cycle test, including the steps of image preprocessing, image import, sub-area setting, correlation analysis and result visualization. It is assumed that the gray distribution of sample subregions before and after deformation is $f(x,y)$ and $g(x',y')$, where x, y and x', respectively represent the position of a feature point before and after deformation, and the correlation coefficient is used to represent the correlation between the target image and the reference image before and after deformation:

$$C = \frac{\sum f(x,y) \times g(x',y')}{\sqrt{\sum f^2(x,y) \times g^2(x',y')}} \quad (1)$$

When $C = 1$, the correlation of subregion before and after deformation is the largest. When $C = 0$, the correlation of subregions before and after deformation is minimum.

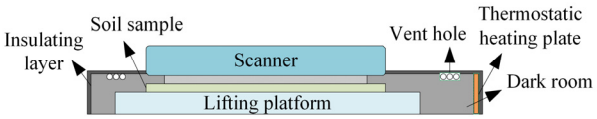

Fig. 1. Diagram of the experimental device.

The molecular regions were divided and adjusted by trial and error method. Since the pixel size of the image studied in this paper was originally 9824×13864, it was reduced to 5457×7582 after high-quality compression, and the subregion size was finally selected to be 40×40 pixels. For each group of samples, the original picture before the wet and dry cycle was taken as the reference image, and the image during the wet and dry cycle was taken as the target image for analysis.

3. Results

3.1. Quantitative index of the crack of the sample surface

The surface crack evolution image of compacted loess obtained in the process of the drying-wetting cycles was extracted by the PCAS system. The main analysis steps include binarization, de-clutter, bridging, skeletonization, etc., and the results are shown in **Fig. 2**.

The total length of cracks increases with the increase of the number of drying-wetting cycles n, as shown in **Fig. 3**. When n = 0 ~ 5, the larger the number of drying-wetting cycles, the larger the average width and fractal dimension of cracks, and slightly decreases when n = 6 or 7. When n = 1, 2, soil cracks begin to occur and network cracks are not formed, and the morphological characteristics of cracks increase rapidly. When n = 3 ~ 5, the development speed of soil surface cracks accelerates rapidly during the drying-wetting cycle. When n = 5, the average width and fractal dimension of soil surface cracks reach the peak value after the drying-wetting cycle, and the average width reaches the maximum value of 11, which is about 4.5 after the drying-wetting cycle, which is about twice as fast as that after the first two drying-wetting cycles. It indicates that the crack expansion degree is the largest and the crack development speed is the fastest. After the fifth drying-wetting cycle, the soil surface cracks showed a healing state to a certain extent by using atomized water spray humidification. When n = 6 or 7, the total length of soil

surface cracks continued to increase, but the expansion degree weakened.

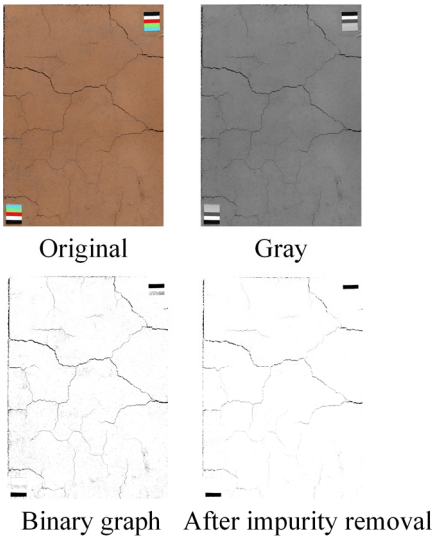

Fig. 2. Diagram of the PCAS system processing process.

At present, it is generally believed that there are several stages of loess fracture development. Some scholars divide the development of loess fracture into three stages: slow, fast, and slow growth [5,7]. Similar rules can also be observed in this experiment. The surface cracks of loess samples can be divided into three stages: in the first two drying-wetting cycles, loess samples are in the stage of the slow development of cracks; During the 3rd ~ 5th drying-wetting cycles, the cracks on the surface of the loess sample were in the stage of rapid growth. During the 6th and 7th drying-wetting cycles, the loess samples were in the slow development stage of cracks.

3.2 Variation of the crack of a sample surface

Limited by space, only part of the pictures are given, as shown in **Fig. 4** and **Fig. 5**. The main strain field is composed of red and blue strips of different lengths and widths, in which the red strip partly represents the tensile strain caused by the soil mass under tensile action, and the blue strip represents the compressive strain caused by the soil mass under shrinkage.

3.2.1. Sample surface crack evolution model

While n = 1, the loess sample is affected by the friction force at the bottom and around the container. In the process of water shrinkage, the surrounding area of the loess sample first detaches from the container, and then cracks occur in the surrounding area and the surface defects of the original sample, as shown in **Fig. 4** (a). However, in the initial dehumidification, the loess sample was structurally complete, so the cracks generated were mostly single cracks without crossing. With the increase of dehumidification time, the existing cracks only increased in length side and width gradually, without differentiation of secondary cracks.

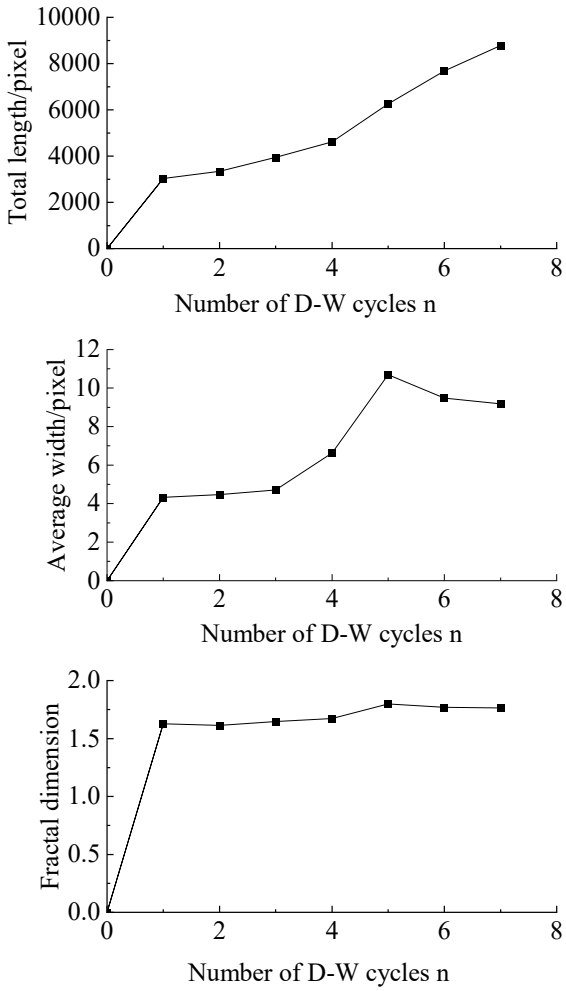

Fig. 3. Surface crack index of loess sample after different drying-wetting cycles.

After the first drying-wetting cycle, the integrity of the loess sample was broken and its structure weakened. In the second dehumidification process of the loess sample, the appearance of existing cracks led to an increase in the number of water loss channels in the loess sample. Micro-cracks began to occur at the early crack location and the boundary of the loess sample, and gradually developed into secondary cracks with the increase of dehumidification time, as shown in **Fig. 5**(c). At the same time, there is a certain Angle between the secondary fissure and the early fissure, and most of them form a "T" shape and a "Y" shape. With the increase of the number of dry and wet cycles, the number of cracks on the surface of the loess sample increases, the total length increases, and the width of cracks widens.

3.2.2. Variation of strain field in the crack of a sample surface

When the loess underwent the first dehumidification process, blue compressive strain distribution was found at the surrounding boundary, which also corresponded to the fact that dry areas first appeared at the boundary in

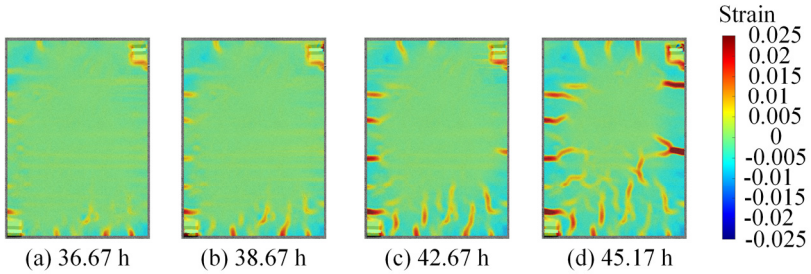

Fig. 4. Principal strain field of loess sample surface during the first dehumidification process.

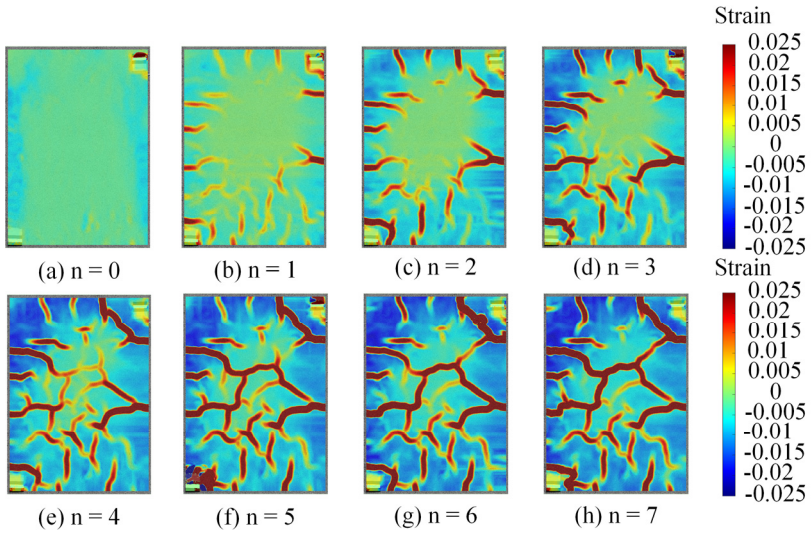

Fig. 5. Principal strain distribution field of loess sample surface after different drying-wetting cycles.

the process of loess water loss, while the central part of the loess was still in a state of high water content. The uneven distribution of water content in the loess led to the appearance of tensile stress, and the loess contracted and compressed at the boundary, resulting in a compressive strain accumulation area. As shown in **Fig. 5** (a), the boundary of the loess mass is separated from the surrounding die. Red bands appear around the original defects of loess and gradually widen and lengthen with the increase of dehumidification time, which is also corresponding to the law of crack development. Red tensile stress appears at the crack position of loess mass, while blue compressive strain area is usually accompanied on both sides. This is because the tensile stress of loess mass gradually increases with the increase of dehumidification time. When the internal tensile stress of loess mass is greater than its own tensile strength, cracks are generated. The width of the crack increases and the loess on both sides is compressed to produce compressive strain. However, the strain generation and development of loess mass are mostly distributed in the area near the existing cracks, while the strain distribution is not found in the central part of loess mass without cracks. When cracks occur, the stress around cracks can be released quickly. The cracks formed in the first dehumidification process often form main cracks, while secondary cracks and micro-cracks are derived from the existing main cracks in the second wet and dry cycle and after. During the humidification process, the cracks on the loess surface heal to varying degrees, and the principal strain on the surface becomes smaller.

3.3. Evolution of cracks of different grades on the sample surface

In order to facilitate the analysis of the changes of cracks of different grades along with the number of drying-wetting cycles on the surface of the loess sample, several characteristic points were selected on the surface of the sample, as shown in **Fig. 6**, to analyze the changes of displacement and strain on behalf of the main cracks, secondary cracks and micro-cracks respectively.

As can be seen from **Fig. 7** and **Fig. 8**, the displacement and strain changes during the development of cracks of different grades on the surface of the soil sample can be divided into three stages: the first stage is n = 1 or 2, with different degrees of displacement occurring at each point on the surface, and the growth rate of the main cracks is the fastest, indicating that the main cracks and a few secondary cracks are mainly developed in this stage, while the development of micro-cracks is less. In the second stage, when n = 2 ~ 5, the displacement of both sides of fractures at all levels increased rapidly, but the increase rate was different. The displacement of the main fracture site increased the most, and the growth rate was also the largest. The increment of the secondary crack is smaller than that of the main crack, while the increment of the micro crack is larger. The peak value was reached at the end of the 5th wet and dry cycle, but the displacement was different at different positions. In the third stage, when n = 6 or 7, the displacement on both sides of cracks at all levels was

smaller than that after the 5th dry-wet cycle, indicating that soil surface cracks were healed to a certain extent after humidification after multiple dry-wet cycles, and the development speed of soil surface cracks slowed down, mainly due to the continuous development of micro-cracks.

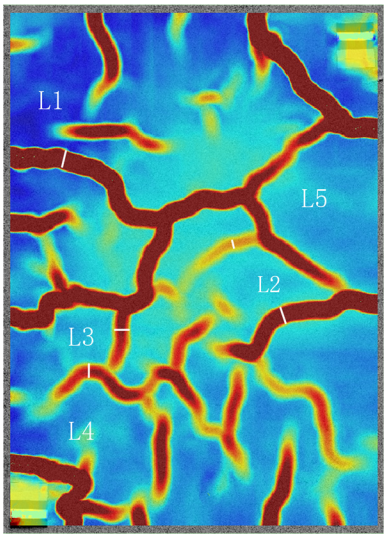

Fig. 6. Surface crack monitoring point of soil sample.

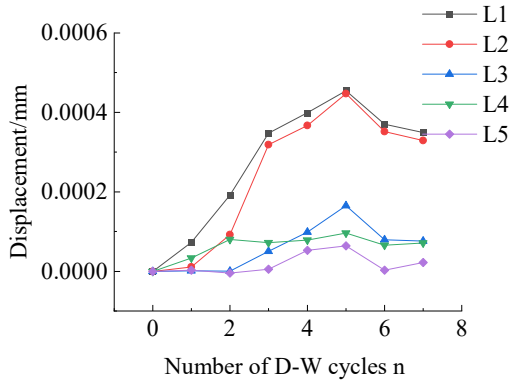

Fig. 7. Displacement curve of different grades of cracks.

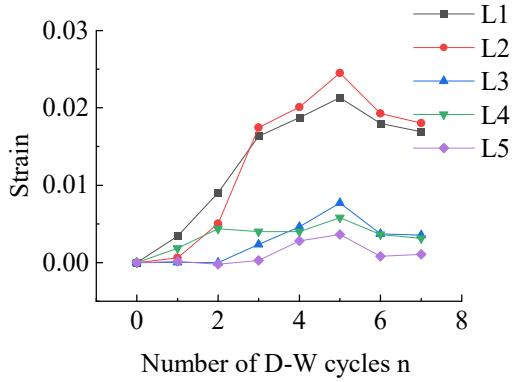

Fig. 8. Strain variation curves of different grades of cracks.

4. Conclusion

(1) The variation of surface crack development in compacted loess samples with the frequency of drying-wetting cycles can be divided into three stages: slow growth stage, rapid growth stage, and sluggish development stage. The total length of loess cracks increases with the increase in the number of wet and dry cycles. The average width and fractal dimension increase with the increase of the number of drying-wetting cycles in the first five cycles, and reach the peak value after the fifth cycle, but decrease slightly during the sixth to seventh cycle.

(2) The distribution of displacement and strain at different locations on the loess surface is different. With the increase of dehumidification time, the tensile strain zone first occurs around the loess and the original defect, and gradually becomes longer and wider. In addition, there are usually compressive strain zones on both sides of cracks.

(3) Loess surface cracks can be divided into primary cracks, secondary cracks, and micro-cracks. The cracks produced in the first two drying-wetting cycles are mostly primary cracks and a few secondary cracks. In the process of the 3rd ~ 5th drying-wetting cycle, the development rates of all levels of cracks were ranked as main cracks, secondary cracks, and micro cracks, and all reached the peak after the 5th drying-wetting cycle. During the 6th ~ 7th drying-wetting cycle, the displacement and strain of fractures at all levels decreased, and the development of primary and secondary fractures slowed down, mainly because of the rapid growth of micro fractures.

(4) DIC technology, as a non-contact rapid and non-destructive measurement means, can intuitively display the changes of full-field surface displacement and strain in the drying-wetting cycling process of loess crack, and provide an effective method for dynamic tracking of the evolution of loess crack and for studying the evolution law and mechanism of loess crack.

References

1. J.D. Liu, C.S Tang, H. Zeng, et al. Evolution of desiccation cracking behavior of clays under drying-wetting cycles. Rock and Soil Mechanics, **42**(10), 2763-2772 (2021)
2. C.S. Tang, Q. Cheng, T. Leng, et al. Effects of wetting-drying cycles and desiccation cracks on mechanical behavior of an unsaturated soil. Catena, **194**, 104721 (2020)
3. T. Li, Y.Q. He, G.K. Liu, et al. Experimental Study on Cracking Behaviour and Strength Properties of an Expansive Soil under Cyclic Wetting and Drying. Shock and Vibration, 2021, 1-13 (2021)
4. K. Li, B. Shi, C.S. Tang, et al. Feasibility research on soil deformation monitoring with distributed optical fiber sensing technique. Rock and Soil Mechanics, **31**(6), 1781-1785 (2010)
5. L. Cao, Z.J. Wang. A Quantitative Analysis System for Morphological Parameters of Surface Desiccation Cracks in Clay. Journal of Yangtze River Scien-tific Research Institute, **31**(4), 63-67,76 (2014)
6. D.X. Hu, X. Li, C.Y. Zhou, et al. Quantitative analysis of swelling and shrinkage cracks in expansive soil. Rock and Soil Mechanics,**39**(S1), 318-324 (2018)

7. L.J. Su, Q. Zhao, H. Liu, et al. Swelling and Shrinkage Behaviors and Evolution Law of Crack Morphology of Undisturbed Loess During Wetting-Drying Cycles. Journal of Tianjin University, **54**(3), 255-267 (2021)
8. C. Zhao, C. Bao, H. Matsuda, et al. Application of digital image correlation method in experimental research on crack propagation of brittle rock. Chinese Journal of Geotechnical Engineering, **37**(5), 944-951 (2015)
9. D.D. Shi, Y.Y. Mao, Y. Yang, et al. Experimental study on the deformation characteristics of soils around uplift circular plate anchors using digital image correlation technology. Rock and Soil Mechanics, **41**(10), 3201-3213 (2020)
10. Y.N. Teng, S. Samuel A, G.Susan M. Synchronised multi-scale image analysis of soil deformations. International Journal of Physical Modelling in Geotechnics, **17**(1), 53-71 (2017)
11. L.L. Wang, C.S. Tang, B. Shi, et al. Nucleation and propagation mechanisms of soil desiccation cracks. Engineering Geology, 238: 27-35 (2018)
12. L. Lin, C.S. Tang, Q. Cheng, et al. Desiccation cracking bebavior of soils based on digital image correlation technique.Chinese Journal of Geotechnical Engineering, **41**(7), 1311-1318 (2019)
13. X. Wei, C.Y. Gao, D.D. Yan, et al. Experimental Study on Cracking Behavior and Mechanism in Desiccating Soils in Xi'an, Shaanxi Province, China. Advances in Civil Engineering, 1-12 (2020)
14. J. Qu, J.L. Ma, B. Yang. Crack initiation and propagation mechanism of earth wall at sanxingdui city. Journal of Engineering Geology, **28**(3), 610-618 (2020)
15. M.T. Zhang, M.L. Wu, A.J. Chen, et al.Experimental study on dry shrinkage cracking of red clay based on DIC technology. Journal of Hunan City University, 30(6), 7-11 (2021)